2019 American Control Conference (ACC)
Philadelphia, PA, USA, July 10-12, 2019

Adaptive Control of Systems with Unknown Nonminimum-Phase Zeros Using Cancellation-Based Pseudo-identification

Syed Aseem Ul Islam, Antai Xie, and Dennis S. Bernstein

***Abstract*— Adaptive control of linear systems with unknown nonminimum-phase (NMP) zeros remains a significant challenge. Although retrospective cost adaptive control (RCAC) is applicable to NMP systems with known NMP zeros, errors in the knowledge of those zeros can lead to unstable pole/zero cancellation under sufficiently aggressive tuning. To address this problem, this paper provides a numerical investigation of a heuristic extension of RCAC that exploits the propensity of RCAC to cancel NMP zeros, thereby inferring the NMP zeros. This modeling information can be subsequently incorporated within the target model used by RCAC. By focusing on only NMP zeros, this approach is distinct from conventional system identification, which relies on input-output data for model fitting. This cancellation-based technique relies on saturation of the control input and instability of the feedback controller. Simultaneous occurrence of control saturation and controller instability provides a heuristic indicator that the controller has cancelled one or more NMP zero during closed-loop operation. The estimated NMP zeros are subsequently used within a *cancellation-based pseudo-identification* extension of RCAC to prevent further cancellation of the NMP zeros.**

I. Introduction

Nonminimum-phase (NMP) zeros represent a fundamental challenge in feedback control of linear systems [1]. These zeros arise from sensor/actuator noncolocation in systems with rotational degrees of freedom [2]. In addition, negative NMP zeros (that is, to the left of -1 on the real axis) arise in sampled-data control of continuous-time systems of relative degree at least three [3].

Beyond fixed-gain control, NMP zeros present an especially significant challenge to adaptive control. Iterative learning control for NMP systems is considered in [4]; approximate inversion techniques are considered in [5], and lifting is applied in [6]. Additional techniques are given in [7], [8], [9], [10], and [11]. Adaptive control of discrete-time NMP systems is considered in [12], [13].

The starting point for the present paper is retrospective cost adaptive control (RCAC). As shown in [14], [15], RCAC is effective for NMP plants assuming that the NMP zeros are either exactly or approximately known. In the case of poorly modeled or unmodeled NMP zeros, RCAC may cancel the NMP zeros, leading to a hidden instability.

A potential solution to the problem of uncertain NMP zeros is to perform either open-loop or closed-loop identification and then extract the estimates of the NMP-zeros [16]. Alternatively, the technique in [17] directly estimates the plant NMP zeros. These and other techniques can be used to estimate the plant NMP zeros, which can then be used by RCAC as an indirect adaptive control method.

As an alternative to identification of NMP zeros, the present paper takes advantage of the propensity of RCAC to cancel NMP zeros. In particular, saturation of the control input along with instability of the feedback controller provide a heuristic indicator of the cancellation of one or more NMP zero during closed-loop operation. The estimated NMP zeros are subsequently used within a *cancellation-based pseudo-identification* extension of RCAC to prevent further cancellation of the NMP zeros.

The contents of the paper are as follows. Section II presents the RCAC algorithm, and Section III gives connections between the RCAC algorithm and NMP plant zeros. In Section IV, we present the cancellation-based pseudo-identification algorithm motivated by Section III. Section V then applies this technique to illustrative examples, which include plants with up to four unknown NMP zeros.

II. Retrospective Cost Adaptive Control

A. Controller Structure

Define the dynamic compensator

$$u(k) = \sum_{i=1}^{\ell_{\mathrm{c}}} P_i(k)u(k-i) + \sum_{i=1}^{\ell_{\mathrm{c}}} Q_i(k)y(k-i), \quad (1)$$

where $P_i(k) \in \mathbb{R}^{l_u \times l_u}$, $Q_i(k) \in \mathbb{R}^{l_u \times l_y}$ are the controller coefficient matrices, and ℓ_{c} is the data-window length. The controller (1) can be recast as

$$u(k) = \Phi(k)\theta(k), \quad (2)$$

where

$$\Phi(k) \triangleq I_{l_u} \otimes \begin{bmatrix} u(k-1) \\ \vdots \\ u(k-\ell_{\mathrm{c}}) \\ y(k-1) \\ \vdots \\ y(k-\ell_{\mathrm{c}}) \end{bmatrix}^{\mathrm{T}} \in \mathbb{R}^{l_u \times l_\theta}, \quad (3)$$

$$\theta(k) \triangleq \mathrm{vec}\begin{bmatrix} P_1(k) \cdots P_{\ell_{\mathrm{c}}}(k)\ Q_1(k) \cdots Q_{\ell_{\mathrm{c}}}(k) \end{bmatrix}^{\mathrm{T}} \in \mathbb{R}^{l_\theta}, \quad (4)$$

where $l_\theta \triangleq l_u^2\ell_{\mathrm{c}} + l_u l_y \ell_{\mathrm{c}}$, "$\otimes$" is the Kronecker product, and "vec" is the column-stacking operator. If y and u are scalar

Syed Aseem Ul Islam, Antai Xie, and Dennis S. Bernstein are with the Department of Aerospace Engineering, University of Michigan, Ann Arbor, MI, USA. {aseemisl, antai, dsbaero}@umich.edu

signals, then the SISO transfer function of the controller from y to u is given by

$$G_{\mathrm{c},k}(\mathbf{q}) = \frac{Q_1(k)\mathbf{q}^{\ell_\mathrm{c}-1} + \cdots + Q_{\ell_\mathrm{c}}(k)}{\mathbf{q}^{\ell_\mathrm{c}} - P_1(k)\mathbf{q}^{\ell_\mathrm{c}-1} - \cdots - P_{\ell_\mathrm{c}}(k)}, \tag{5}$$

where $\mathbf{q}$ is the forward-shift operator.

B. Retrospective Performance

The retrospective performance variable is defined as

$$\hat{z}(k,\hat{\theta}) \triangleq z(k) - G_\mathrm{f}(\mathbf{q})[u(k) - \hat{u}(k)], \tag{6}$$

where

$$\hat{u}(k) \triangleq \Phi(k)\hat{\theta}, \tag{7}$$

$z(k), \hat{z}(k) \in \mathbb{R}^{l_z}$, $\hat{u}(k) \in \mathbb{R}^{l_u}$, and $\hat{\theta} \in \mathbb{R}^{l_\theta}$ is determined by the optimization below. The rationale underlying (6) is to replace the actual past control inputs with retrospectively optimized control inputs $\hat{u}(k)$.

The $n_z \times n_u$ finite-impulse-response filter G_f of order n_f has the form

$$G_\mathrm{f} \triangleq \sum_{i=1}^{n_\mathrm{f}} N_i \mathbf{q}^{-i}, \tag{8}$$

where each N_i is an $l_z \times l_u$ matrix. We can rewrite (6) as

$$\hat{z}(k,\hat{\theta}) \triangleq z(k) - N[\bar{U}(k) - \bar{\Phi}(k)\hat{\theta}], \tag{9}$$

where

$$N \triangleq \left[\begin{array}{ccc} N_1 & \cdots & N_{n_\mathrm{f}} \end{array}\right] \in \mathbb{R}^{l_z \times n_\mathrm{f} l_u}, \tag{10}$$

$$\bar{\Phi}(k) \triangleq \left[\begin{array}{c} \Phi(k-1) \\ \vdots \\ \Phi(k-n_\mathrm{f}) \end{array}\right] \in \mathbb{R}^{n_\mathrm{f} l_u \times l_\theta}, \tag{11}$$

$$\bar{U}(k) \triangleq \left[\begin{array}{c} u(k-1) \\ \vdots \\ u(k-n_\mathrm{f}) \end{array}\right] \in \mathbb{R}^{n_\mathrm{f} l_u}. \tag{12}$$

C. Retrospective Cost

Using the retrospective performance variable $\hat{z}(k,\hat{\theta})$ defined by (6), we define the cumulative retrospective cost function

$$J(k,\hat{\theta}) \triangleq \sum_{i=0}^{k} [\hat{z}^\mathrm{T}(i,\hat{\theta})\hat{z}(i,\hat{\theta}) + (\Phi(i)\hat{\theta})^\mathrm{T} R_u \Phi(i)\hat{\theta}] + [\hat{\theta} - \theta(0)]^\mathrm{T} P(0)[\hat{\theta} - \theta(0)], \tag{13}$$

where $P(0)$ is positive definite and R_u is positive semidefinite. The following result uses recursive least squares to minimize (13); the minimizer $\hat{\theta}_\mathrm{min}$ of (13) is used to update the controller coefficient vector $\theta(k)$, that is, $\theta(k+1) \triangleq \hat{\theta}_\mathrm{min}$.

Proposition: Let $P(0)$ and R_u be positive definite. Then, for all $k \geq 0$, the retrospective cost function (13) has the unique global minimizer $\theta(k+1)$ given by

$$P(k+1) = P(k)[I_{l_\theta} - \gamma^\mathrm{T}(k)\beta(k)\gamma(k)P(k)], \tag{14}$$

$$\theta(k+1) = \theta(k) - P(k+1)\gamma^\mathrm{T}(k)\bar{R}\psi(k), \tag{15}$$

where

$$\beta(k) \triangleq [\bar{R}^{-1} + \gamma(k)P(k)\gamma^\mathrm{T}(k)]^{-1}, \tag{16}$$

$$\gamma(k) \triangleq \left[\begin{array}{c} N\bar{\Phi}(k) \\ \Phi(k) \end{array}\right], \quad \bar{R} \triangleq \left[\begin{array}{cc} I_{l_z} & 0_{l_z \times l_u} \\ 0_{l_u \times l_z} & R_u \end{array}\right], \tag{17}$$

$$\psi(k) \triangleq \left[\begin{array}{c} N\bar{\Phi}(k)\theta(k) + z(k) - N\bar{U}(k) \\ \Phi(k)\theta(k) \end{array}\right]. \tag{18}$$

Finally, the control input at step k is given by

$$u(k) = \Phi(k)\theta(k). \tag{19}$$

For all numerical examples below, the controller coefficient is initialized as $\theta(0) = 0_{l_\theta \times 1}$ in order to reflect the absence of additional prior modeling information. The matrices $P(0)$ and R_u are chosen to tune the rate of adaptation, and are fixed for all simulations.

III. RCAC and NMP zeros

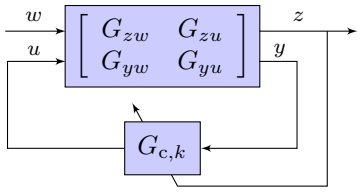

Fig. 1. Block diagram of the adaptive standard problem. w is the exogenous signal of commands and disturbances, z is the performance variable which is used to adapt the controller, y is the measurement that drives the controller, and u is the control signal. The coefficients of the linear controller $G_{\mathrm{c},k}$ are updated at each time step k.

In the context of the adaptive standard problem shown in Figure 1, it is shown in [15] that RCAC may cancel NMP zeros of the transfer function G_{zu} that are not modeled by the target model G_f. To state this property, let G_c^* denote the asymptotic controller arising from the adaptation, and define the notation

$$G_\mathrm{f} \triangleq \frac{N_\mathrm{f}}{\mathbf{q}^{n_\mathrm{f}}}, \; G_{zu} \triangleq \frac{N_{zu}}{D}, \; G_{yu} \triangleq \frac{N_{yu}}{D}, \; G_\mathrm{c}^* \triangleq \frac{N_\mathrm{c}^*}{D_\mathrm{c}*}. \tag{20}$$

Then, it can be seen from (6) that optimization of (13) implies that $z(k) \approx G_\mathrm{f}(\mathbf{q})\tilde{u}$, where $\tilde{u} \triangleq u(k) - \hat{u}(k)$. The effect of this optimization is thus to match the closed-loop transfer function from $\tilde{u}$ to $z(k)$ to the filter G_f. As shown in [15], the closed-loop transfer function from $\tilde{u}$ to $z(k)$ is given by the intercalated transfer function defined by

$$\tilde{G}_{z\tilde{u}}^*(\mathbf{q}) = \frac{N_{zu}(\mathbf{q})\mathbf{q}^{\ell_\mathrm{c}}}{D(\mathbf{q})D_\mathrm{c}^*(\mathbf{q}) - N_{yu}(\mathbf{q})N_\mathrm{c}^*(\mathbf{q})}, \tag{21}$$

$$= \frac{N_{zu}(\mathbf{q})\mathbf{q}^{\ell_\mathrm{c}}}{D_\mathrm{c}^*(\mathbf{q})\left[D(\mathbf{q}) - \frac{N_{yu}(\mathbf{q})N_\mathrm{c}^*(\mathbf{q})}{D_\mathrm{c}^*(\mathbf{q})}\right]}. \tag{22}$$

Consequently, G_f serves as a target model for the intercalated transfer function $\tilde{G}_{z\tilde{u}}^*$.

In the case where $G_{zu} \neq G_{yu}$, it can be seen from (21) that roots of N_{zu} that are not present in N_f may be cancelled by closed-loop poles, which are the roots of $DD_\mathrm{c}^* - N_{yu}N_\mathrm{c}^*$. Alternatively, in the case where $G_{zu} = G_{yu}$, it can be seen from (22) that roots of N_{zu} that are not present in N_f may be cancelled by controller poles, which are the roots of $D_\mathrm{c}^*(\mathbf{q})$.

To illustrate non-cancellation and cancellation of modeled and unmodeled NMP zeros of G, respectively, we consider a broadband disturbance rejection problem for the NMP plant $G = G_{zu} = G_{yu}$ given by

$$G(\mathbf{q}) = \frac{\mathbf{q} - 1.3}{\mathbf{q}^2 - 0.7\mathbf{q} + 0.48}, \tag{23}$$

which has a real NMP zero at 1.3 rad/sample, and $G_{zw} = G_{yw} = \begin{bmatrix} -1 & G \end{bmatrix}$. In the notation of Section V, $d(k) \sim N(0, 0.1^2)$, $\ell_{\mathrm{c}} = 10$, $P(0) = 100 I_{l_\theta}$, and $R_u = 0$.

First, we exactly model the NMP zero of G in the target model G_{f} by setting $G_{\mathrm{f}}(\mathbf{q}) = \frac{\mathbf{q}-1.3}{\mathbf{q}^2}$. In this case RCAC rejects the disturbance, and the asymptotic controller $G_{\mathrm{c},\infty}$ does not cancel the NMP zero of G, as shown in Figure 2. Next, we consider the case where the NMP zero of G is erroneously modeled by G_{f}, and we determine the largest value of P_0, where $P(0) = P_0 I_{l_\theta}$, for which RCAC does not cancel the NMP zero. To do this, we set $G_{\mathrm{f}}(\mathbf{q}) = \frac{\mathbf{q}-\alpha_{\mathrm{z}}}{\mathbf{q}^2}$ and vary α_{z} between 1.05 and 3, with the true NMP zero fixed at 1.3 rad/sample. The maximum value of P_0 versus α_{z} is shown in Figure 3. As expected, RCAC is most robust to P_0 in the case where the NMP zero of G is exactly modeled by G_{f}. For larger values of P_0, RCAC is sufficiently aggressive to cancel the NMP zero.

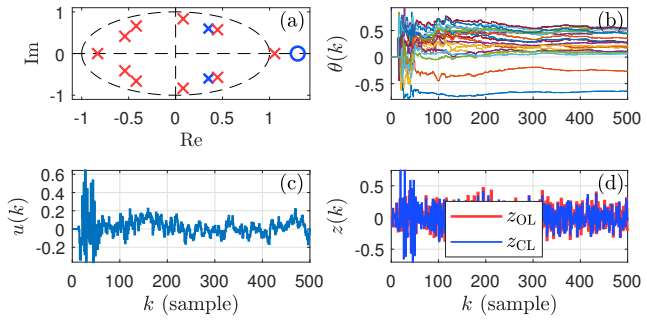

Fig. 2. Broadband disturbance rejection with the NMP zero exactly modeled by G_{f}. (a) shows the poles and zeros of G as well as the poles of the asymptotic controller $G_{\mathrm{c},\infty}$ with blue crosses and circles, and red crosses, respectively; (b) shows the controller coefficients θ; (c) shows the control u; and (d) shows the open- and closed-loop responses.

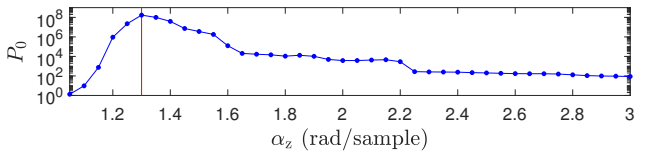

Fig. 3. Maximum value of P_0, where $P(0) = P_0 I_{l_\theta}$, for which the asymptotic controller $G_{\mathrm{c},\infty}$ does not cancel the NMP zero of G, versus the location of the zero of G_{f}. The vertical red line shows the location of the NMP zero of G.

Next, we set $G_{\mathrm{f}}(\mathbf{q}) = \frac{1}{\mathbf{q}}$, and thus the NMP zero of G is not modeled either exactly or erroneously in G_{f}. In this case the asymptotic controller $G_{\mathrm{c},\infty}$ cancels the NMP zero of G with a controller pole as shown in Figure 4 with $P(0) = 100 I_{l_\theta}$. Accordingly, the control u and error z diverge. Additionally, we investigate the effect of a magnitude saturation on the control u in the case where the NMP zero of G is not modeled by G_{f}. With control saturation ± 20, Figure 5 shows that the asymptotic controller $G_{\mathrm{c},\infty}$ cancels the NMP zero of G, but the control u is bounded due to the saturation. With control saturation ± 0.1, which severely limits the control input, Figure 6 shows that the asymptotic controller $G_{\mathrm{c},\infty}$ is prevented from canceling the NMP zero of G. Note that, in Figures 5-6, which correspond to cases with control saturation, the controller coefficient vector θ converges. Figure 7 shows the distance between the right-half plane real pole of the asymptotic controller $G_{\mathrm{c},\infty}$ and the NMP zero of G versus the control saturation level. Figure 7 shows that a smaller saturation level yields a larger pole-zero distance. In particular, for this example, saturation levels smaller than 10^{-2} severely restrict the ability of RCAC to place a pole at the NMP zero of G. Conversely, a larger saturation level yield a smaller pole-zero distance.

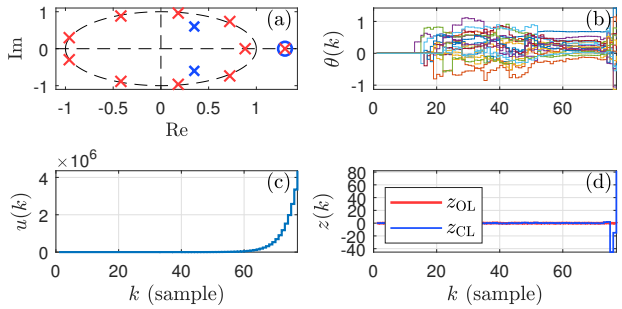

Fig. 4. Cancellation of the unmodeled NMP zero of G. (a) shows the poles and zeros of G as well as the poles of the asymptotic controller $G_{\mathrm{c},\infty}$ with blue crosses and circles, and red crosses, respectively; (b) shows the controller coefficients θ; (c) shows the control u; and (d) shows the open- and closed-loop responses. The NMP zero of G is cancelled by $G_{\mathrm{c},\infty}$, and, as a result, u and z diverge.

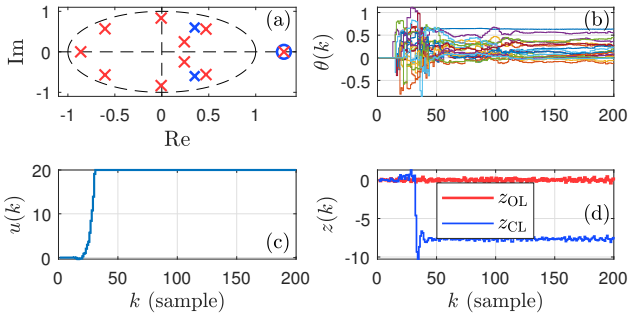

Fig. 5. Cancellation of the unmodeled NMP zero of G in the presence of control saturation. (a) shows the poles and zeros of G as well as the poles of the asymptotic controller $G_{\mathrm{c},\infty}$ with blue crosses and circles, and red crosses, respectively; (b) shows the controller coefficients θ; (c) shows the control u saturated at ± 20; and (d) shows the open- and closed-loop responses. The NMP zero of G is cancelled by $G_{\mathrm{c},\infty}$, but u and z remain bounded due to the saturation on u. In addition, θ converges.

In this paper we consider problems with $G = G_{zu} = G_{yu}$; in this case, the NMP zeros of G_{zu} that are not modeled by G_{f} are in the feedback loop and thus may be cancelled by unstable controller poles as shown in (22). The control u diverges in the case where a controller pole cancels a NMP plant zero. Unbounded growth of u is, of course, prevented by control saturation, which is present in all realistic applications. Control saturation in the case of unstable pole-zero cancellation also leads to convergence of θ, and thus convergence of the controller poles. Finally, the converged locations of the unstable poles of $G_{\mathrm{c},\infty}$ can be used to estimate the NMP zeros of G. This is the motivation for the algorithm described in the next section.

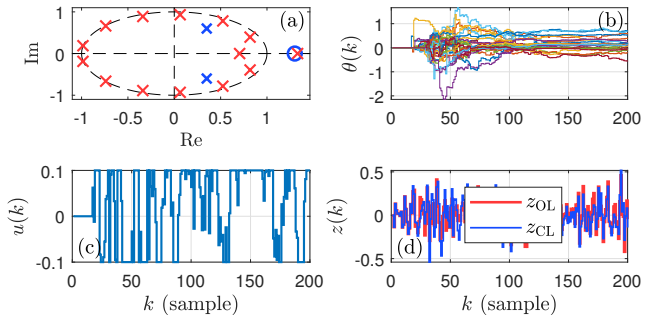

Fig. 6. Cancellation of the unmodeled NMP zero of G in the presence of control saturation. (a) shows the poles and zeros of G as well as the poles of the asymptotic controller $G_{\mathrm{c},\infty}$ with blue crosses and circles, and red crosses, respectively; (b) shows the controller coefficients θ; (c) shows the control u saturated at ± 0.1; and (d) shows the open- and closed-loop responses. The NMP zero of G is approximately canceled by $G_{\mathrm{c},\infty}$, and u and z remain bounded. In addition, θ converges.

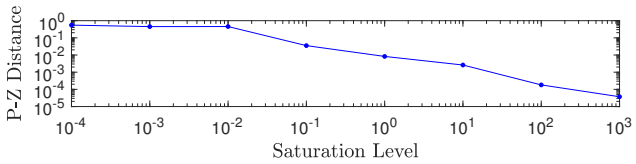

Fig. 7. Distance between the rightmost real pole of the asymptotic controller $G_{\mathrm{c},\infty}$ and the NMP zero of G versus the saturation level for u. The pole of $G_{\mathrm{c},\infty}$ is closer to the NMP zero of G as the saturation level increases.

IV. Cancellation-Based Pseudo-Identification

In this section we present the cancellation-based pseudo-identification (CBPI) algorithm. We consider plants that are either Lyapunov stable or asymptotically stable and whose NMP zeros have magnitude greater than 1.05. As in [15], it is assumed that the relative degree and sign of the leading numerator coefficient of the plant are known.

To implement CBPI, (19) is modified as

$$u(k) \triangleq \mathrm{sat}_{\alpha}[\Phi(k)\theta(k)], \tag{24}$$

where

$$\mathrm{sat}_{\alpha}(x) = \begin{cases} x, & |x| \leq \alpha, \\ \alpha \mathrm{sign}(x), & \text{otherwise}, \end{cases} \tag{25}$$

is an artificial control saturation level implemented as part of the control algorithm. The artificial control saturation level is chosen to be smaller than the actual actuator saturation, which is determined by the physical constraints on the actuator. We define the saturation counter for $k > 0$

$$n_{\alpha}(k) \triangleq \begin{cases} n_{\alpha}(k-1)+1, & |\phi(k)\theta(k)| > \alpha, \\ n_{\alpha}(k-1), & \text{otherwise}, \end{cases} \tag{26}$$

which counts the number of steps in which the magnitude $|\phi(k)\theta(k)|$ of the requested control is greater than the saturation level α. The step k_{conv} is the smallest step $k > 2\ell_{\mathrm{c}}$ such that $n_{\alpha}(k) > n_{\alpha,\max}$ and such that the vector of denominator coefficients θ_{den} has approximately converged, that is,

$$\left\| \theta_{\mathrm{den}}(k_{\mathrm{conv}}) - \frac{1}{\ell_{\mathrm{c}}} \sum_{i=k_{\mathrm{conv}}-\ell_{\mathrm{c}}}^{k_{\mathrm{conv}}} \theta_{\mathrm{den}}(i) \right\| < \varepsilon, \tag{27}$$

where ε is a convergence threshold, and $n_{\alpha,\max}$ is the saturation counter threshold.

RCAC is implemented with the modified controller output (24), and for $k \leq k_{\mathrm{conv}}$ the target model $G_{\mathrm{f}}(\mathbf{q}) = \frac{1}{\mathbf{q}}$ is used. At step $k = k_{\mathrm{conv}}$, the target model G_{f} is modified. In particular, for all $k > k_{\mathrm{conv}}$, G_{f} is set to a finite-impulse response filter with zeros at the locations of all poles of $G_{\mathrm{c},k_{\mathrm{conv}}}$ that have spectral radius greater than 1.05. Furthermore, at step $k = k_{\mathrm{conv}}$, $P(k)$ and $\theta(k)$ are reinitialized to $P(0)$ and $0_{l_\theta \times 1}$, respectively. The parameters $\alpha, n_{\alpha,\max}$, and ε completely specify the CPBI algorithm.

V. Numerical Examples

Consider a single-input, single-output (SISO) plant

$$x(k+1) = Ax(k) + Bu(k) + Bd(k), \tag{28}$$

$$y_0(k) = Cx(k) + v(k), \tag{29}$$

$$z(k) \triangleq y_0(k) - r(k), \tag{30}$$

where $x(k) \in \mathbb{R}^n$ is the state, $u(k) \in \mathbb{R}$ is the control input, $d(k) \in \mathbb{R}$ is the disturbance, $y_0(k) \in \mathbb{R}$ is plant output, $r(k) \in \mathbb{R}$ is the command, $v(k) \in \mathbb{R}$ is the sensor noise, and $z(k) \in \mathbb{R}$ is the measured error, which is also the performance variable. For each example, we obtain a minimal realization of the discrete-time transfer function given in terms of $\mathbf{q}$. The realization (A, B, C) with the initial condition $x(0) = 0$ is used for all numerical examples.

For all examples, let $\ell_{\mathrm{c}} = 16$, $P(0) = 10I_{l_\theta}$, $R_u = 0$, and $v(k) \sim N(0, 0.01^2)$ to model sensor noise. For CBPI, we set $\alpha = 4, n_{\alpha,\max} = 10$, and $\varepsilon = 0.01$. No attempt is made to refine either the RCAC weightings or the CBPI parameters for each example.

Example 1. *Step command following with one real NMP zero.* Consider the NMP system

$$G(\mathbf{q}) = \frac{\mathbf{q} - 1.4}{\mathbf{q}^2 - 0.7\mathbf{q} + 0.61}, \tag{31}$$

with one NMP zero at 1.4 rad/sample, and the command

$$r(k) = \begin{cases} 1, & k \leq 300, \\ -1, & k > 300. \end{cases} \tag{32}$$

We apply RCAC/CBPI for $0 \leq k \leq 500$. Figure 8 shows that at $k = 64$ RCAC places a real controller pole at the location of the real NMP zero of G. At $k = 64$, CBPI modifies G_{f} by including the real NMP zero of G in G_{f}. Figure 9 shows the command following performance of RCAC with CBPI. RCAC follows the multi-step command asymptotically. $\diamond$

Example 2. *Harmonic command following with a pair of complex NMP zeros.* Consider the NMP system

$$G(\mathbf{q}) = \frac{(\mathbf{q} - 0.43)(\mathbf{q}^2 - 2.1\mathbf{q} + 1.26)}{(\mathbf{q} - 0.1)(\mathbf{q} - 0.2)(\mathbf{q}^2 - 1.2\mathbf{q} + 0.61)}, \tag{33}$$

with a pair of complex NMP zeros at $\{1.05 \pm 0.4\jmath\}$ rad/sample, and the command $r(k) = \sin 0.13k$. We apply RCAC/CBPI for $0 \leq k \leq 500$. Figure 10 shows that at $k = 99$ RCAC places a pair of complex controller poles

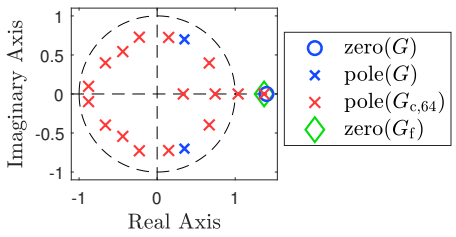

Fig. 8. Example 1: Pseudo-identification of the NMP zero of G. The poles and zeros of G, the poles of $G_{c,64}$, and the zeros of G_f at $k = 64$ are plotted as shown. One NMP zero of G is identified by CBPI and subsequently modeled by G_f.

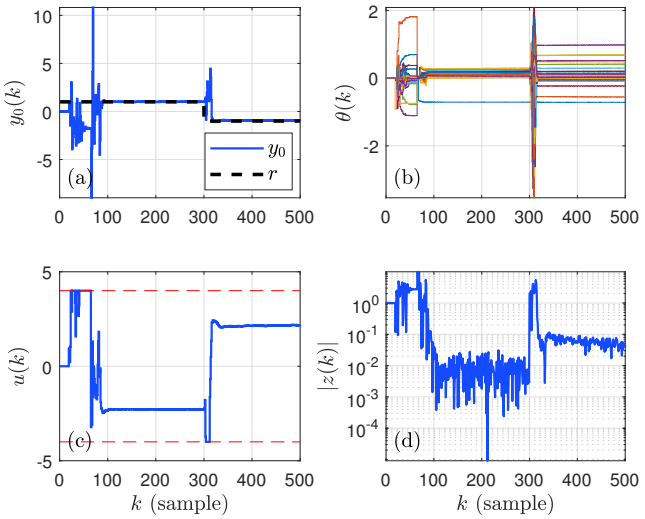

Fig. 9. Example 1: Step command following for a NMP system. (a) shows the command following performance; (b) shows the controller coefficients θ, which readapt in response to the change in command; (c) shows the control u, which is saturated at ± 4; and (d) shows the command-following error on a log scale.

at the locations of the complex NMP zeros of G. At $k = 99$, CBPI modifies G_f by including the pair of complex NMP zeros of G in G_f. Figure 11 shows the command following performance of RCAC with CBPI. RCAC follows the harmonic command asymptotically. ◇

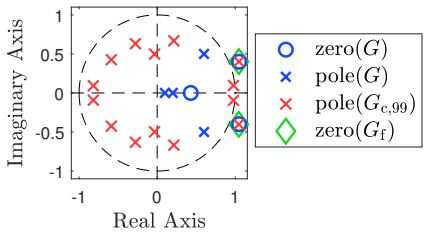

Fig. 10. Example 2: Pseudo-identification of the NMP zeros of G. The poles and zeros of G, the poles of $G_{c,99}$, and the zeros of G_f at $k = 99$ are plotted as shown. Two NMP zeros of G are identified by CBPI and subsequently modeled by G_f.

Example 3. *Harmonic disturbance rejection with a negative NMP zero and a pair of complex NMP zeros.* Consider the NMP system

$$G(\mathbf{q}) = \frac{(\mathbf{q}+1.4)(\mathbf{q}^2-1.6\mathbf{q}+1.13)}{(\mathbf{q}-0.05)(\mathbf{q}-0.25)(\mathbf{q}^2-\mathbf{q}+0.61)}, \qquad (34)$$

with three NMP zeros at $\{-1.4, 0.8 \pm 0.7\jmath\}$ rad/sample, and the disturbance $d(k) = 0.1 \sin 0.234k$. We apply RCAC/CBPI for $0 \le k \le 500$. Figure 12 shows that $G_{c,87}$

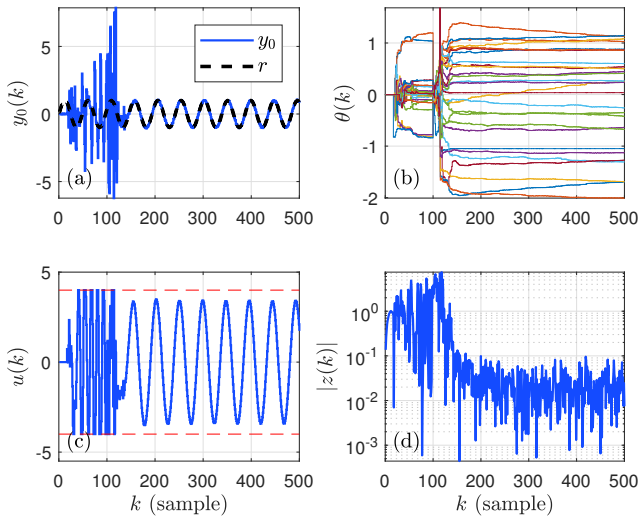

Fig. 11. Example 2: Harmonic command following for a NMP system. (a) shows the command following performance; (b) shows the controller coefficients θ; (c) shows the control u, which is saturated at ± 4; and (d) shows the command-following error on a log scale.

has one real pole and a pair of complex poles at the locations of the real and complex NMP zeros of G. At $k = 87$, CBPI modifies G_f by including the real NMP zero pair of complex NMP zeros of G in G_f. Figure 13 shows the disturbance rejection performance of RCAC with CBPI. RCAC rejects the harmonic disturbance asymptotically. ◇

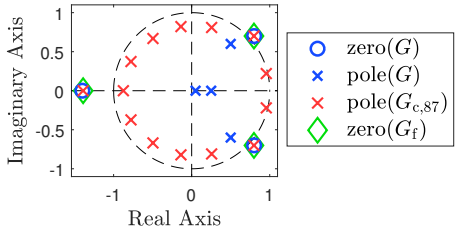

Fig. 12. Example 3: Pseudo-identification of the NMP zeros of G. The poles and zeros of G, the poles of $G_{c,87}$, and the zeros of G_f at $k = 87$ are plotted as shown. Three NMP zeros of G are identified by CBPI and subsequently modeled by G_f.

Example 4. *Broadband disturbance rejection with four complex NMP zeros.* Consider the NMP system

$$G(\mathbf{q}) = \frac{(\mathbf{q}^2-2.2\mathbf{q}+1.37)(\mathbf{q}^2-1.1\mathbf{q}+1.21)}{(\mathbf{q}-0.5)(\mathbf{q}^2-1.6\mathbf{q}+0.76)(\mathbf{q}^2-0.5\mathbf{q}+0.93)}, \qquad (35)$$

with four NMP zeros at $\{0.55 \pm 0.95\jmath, 1.1 \pm 0.4\jmath\}$ rad/sample, and the disturbance $d(k) \sim N(0, 0.1^2)$. We apply RCAC/CBPI for $0 \le k \le 2000$. Figure 14 shows that at $k = 631$ RCAC places four complex controller poles at the locations of the four complex NMP zeros of G. At $k = 631$, CBPI modifies G_f by including the four complex NMP zeros of G in G_f. Figure 15 shows the disturbance rejection performance of RCAC with CBPI. RCAC rejects the broadband disturbance asymptotically. ◇

VI. Conclusions

This paper presented a novel cancellation-based psuedo-identification technique for adaptive control of nonminimum phase (NMP) plants with unknown NMP zeros. This method

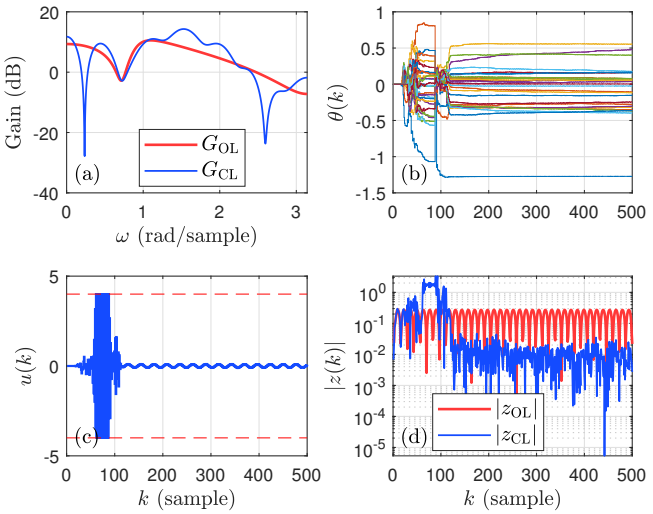

Fig. 13. Example 3: Harmonic disturbance rejection for a NMP system. (a) shows the open- and closed-loop frequency response; (b) shows the controller coefficients θ; (c) shows the control u, which is saturated at ± 4; and (d) shows the open- and closed-loop disturbance rejection errors.

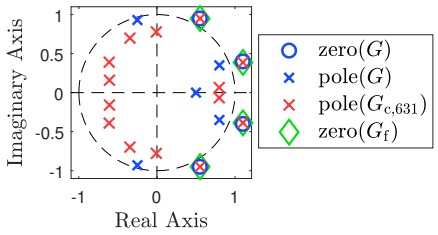

Fig. 14. Example 4: Pseudo-identification of the NMP zeros of G. The poles and zeros of G, the poles of $G_{\rm c,631}$, and the zeros of $G_{\rm f}$ at $k = 631$ are plotted as shown. Four NMP zeros of G are identified by CBPI and subsequently modeled by $G_{\rm f}$.

is based on exploiting the propensity of the RCAC controller to cancel the NMP zeros of the plant while restricting the control output u with control saturation. When cancellation occurs, the unstable controller poles coincide with the NMP zeros of the plant. These unstable poles are subsequently modeled by $G_{\rm f}$ to enable adaptive control of the NMP plant. With severely limited modeling information, this heuristic extension of RCAC was demonstrated for step and harmonic command following as well as for harmonic and broadband disturbance rejection problems on plants with up to four unmodeled NMP zeros. For all numerical examples, no attempt was made to retune either the CBPI algorithm or the RCAC weightings. Future research will investigate the efficacy of CBPI with composite FIR-IIR controllers [18] as well as application to unstable plants.

VII. Acknowledgments

Supported by the Office of Naval Research under grant N00014-18-1-2211 of the BRC Program and by the National Science Foundation under grant CMMI-1634709.

References

[1] J. B. Hoagg and D. S. Bernstein, "Nonminimum-Phase Zeros: Much to Do about Nothing," *IEEE Contr. Sys. Mag.*, vol. 27, no. June, pp. 45–57, 2007.

[2] A. V. Morozov, J. B. Hoagg, and D. S. Bernstein, "Retrospective adaptive control of a planar multilink arm with nonminimum-phase zeros," in *Proc. Conf. Dec. Contr.*, Atlanta, GA, December 2010, pp. 3706–3711.

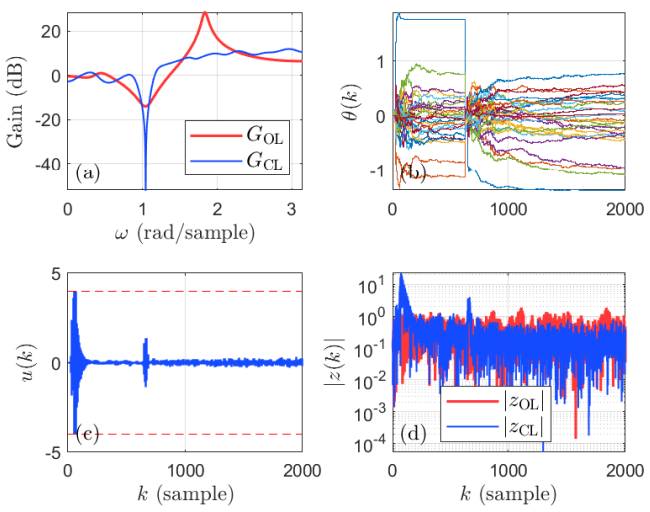

Fig. 15. Example 4: Broadband disturbance rejection for a NMP system. (a) shows the open- and closed-loop frequency response; (b) shows the controller coefficients θ; (c) shows the control u, which is saturated at ± 4; and (d) shows the open- and closed-loop disturbance rejection errors.

[3] K. J. Astrom and B. Wittenmark, *Computer-Controlled Systems: Theory and Design*, 3rd ed. Prentice-Hall, 1996.

[4] J. Ghosh and B. Paden, "Iterative Learning Control for Nonlinear Nonminimum Phase Plants," *J. Dyn. Sys. Meas. Contr.*, vol. 123, pp. 21–30, 2006.

[5] B. P. Rigney, L. Y. Pao, and D. A. Lawrence, "Nonminimum phase dynamic inversion for settle time applications," *IEEE Trans. Contr. Sys. Tech.*, vol. 17, pp. 989–1005, 2009.

[6] D. S. Bayard, "Extended Horizon Liftings for Stable Inversion of Nonminimum-Phase Systems," *IEEE Trans. Autom. Contr.*, vol. 39, pp. 1333–1338, 1994.

[7] J. Kim and K. Choi, "Direct Adaptive Control with Integral Action for Nonminimum Phase Systems," *IEEE Trans. Autom. Contr.*, vol. AC-32, no. 5, pp. 438–442, 1987.

[8] R. Lozano, A. Osorio, and J. Torres, "Adaptive Stabilization of Nonminimum Phase First-Order Continuous-Time Systems," *IEEE Trans. Autom. Contr.*, vol. 39, no. 8, pp. 1748–1751, 1994.

[9] M. C. Campi, "Adaptive Control of Nonminimum Phase Systems," *Int. J. Adaptive Contr. Signal Proc.*, vol. 9, no. 2, pp. 137–149, 1995.

[10] D. A. Suárez and R. Lozano, "Adaptive Control of Nonminimum Phase Systems Subject to Unknown Bounded Disturbances," *IEEE Trans. Autom. Contr.*, vol. 41, no. 12, pp. 1830–1836, 1996.

[11] Z. Lin and G. Tao, "Adaptive Control of a Weakly Nonminimum Phase Linear System," *IEEE Trans. Autom. Contr.*, vol. 45, no. 4, pp. 824–829, 2000.

[12] G. C. Goodwin and K. S. Sin, "Adaptive Control of Nonminimum Phase Systems," *IEEE Trans. Autom. Contr.*, vol. 26, pp. 478–483, 1981.

[13] J. Lu and T. Yahagi, "Discrete-time Model Reference Adaptive Control for Nonminimum Phase Systems with Disturbances Using Approximate Inverse Systems," *IEE Proc.-Control Theory Appl.*, vol. 144, no. 5, pp. 447–454, 1997.

[14] J. B. Hoagg and D. Bernstein, "Retrospective Cost Model Reference Adaptive Control for Nonminimum-Phase Systems," *AIAA J. Guid. Contr. Dyn.*, vol. 35, pp. 1767–1786, 2012.

[15] Y. Rahman, A. Xie, and D. S. Bernstein, "Retrospective Cost Adaptive Control: Pole Placement, Frequency Response, and Connections with LQG Control," *IEEE Contr. Sys. Mag.*, vol. 37, pp. 28–69, Oct. 2017.

[16] F. M. Sobolic, K. F. Aljanaideh, and D. S. Bernstein, "A Numerical Investigation of Direct and Indirect Closed-Loop Architectures for Estimating Nonminimum-Phase Zeros," *Int. J. Contr.*, pp. 1–15, 2018.

[17] C. R. Rojas, H. Hjalmarsson, L. Gerencser, and J. Martensson, "Consistent estimation of real NMP zeros in stable LTI systems of arbitrary complexity," in *Proc. SYSID 2009*, Saint-Malo, France, July 2009, pp. 922–927.

[18] Y. Rahman, K. F. Aljanaideh, and D. S. Bernstein, "Retrospective Cost Adaptive Control Using Composite FIR/IIR Controllers," in *Proc. Amer. Contr. Conf.*, Milwaukee, WI, June 2018, pp. 893–898.